Reference transcriptome data in silkworm *Bombyx mori*

Kakeru Yokoi[1,2,*,**], Takuya Tsubota[3,*], Akiya Jouraku[1], Hideki Sezutsu[3], Hidemasa Bono[4,5]

1 Insect Genome Research and Engineering Unit, Division of Applied Genetics, Institute of Agrobiological Sciences (NIAS), National Agriculture and Food Research Organization (NARO), 1-2 Owashi, Tsukuba, Ibaraki 305-8634, Japan

2 Research Center for Agricultural Information Technology (RCAIT), National Agriculture and Food Research Organization (NARO), Kintetsu Kasumigaseki Building Kasumigaseki 3-5-1 Chiyoda-ku, Tokyo 100-0013, Japan

3 Transgenic Silkworm Research Unit, Division of Biotechnology, Institute of Agrobiological Sciences (NIAS), National Agriculture and Food Research Organization (NARO), 1-2 Owashi, Tsukuba, Ibaraki 305-8634, Japan

4 Database Center for Life Science (DBCLS), Joint Support-Center for Data Science Research, Research Organization of Information and Systems, 1111 Yata, Mishima, Shizuoka 411-8540, Japan

5 Program of Biomedical Science, Graduate School of Integrated Sciences for Life, Hiroshima University, 3-10-23 Kagamiyama, Higashi-Hiroshima city, Hiroshima, 739-0046, Japan

*These authors equally contributed to this work.

**Corresponding author: Kakeru Yokoi

E-mail addresses

Kakeru Yokoi: yokoi123@affrc.go.jp

Takuya Tsubota: tsubota@affrc.go.jp

Akiya Jouraku: joraku@affrc.go.jp

Hideki Sezutsu: hsezutsu@affrc.go.jp

Hidemasa Bono: bonohu@hiroshima-u.ac.jp

Abstract

Background:

The silkworm *Bombyx mori* is a lepidopteran model insect with biological and industrial importance. Its high-quality genome sequence has recently become available and the utilization of this information in combination with extensive transcriptomic analyses is expected to provide an elaborate gene model. It will also be possible to clarify gene expression in detail using this approach.

Results:

We herein performed RNA-seq analysis of ten major tissues/subparts of silkworm larvae. Sequences were mapped onto the reference genome assembly and reference transcriptome data was successfully constructed. The reference data provided a nearly complete sequence for *sericin-1*, a major silk gene with a complex structure. We also markedly improved the gene model for other genes. Transcriptomic expression was investigated in each tissue and a number of transcripts were identified that were exclusively expressed in tissues such as the testis. Transcripts strongly expressed in the midgut formed tight genomic clusters, suggesting that they originated from tandem gene duplication. Transcriptional factor genes expressed in specific tissues or the silk gland subparts were also identified.

Conclusions:

We successfully constructed reference transcriptome data in the silkworm and found that a number of transcripts showed unique expression profiles. These results will facilitate basic studies on the silkworm and accelerate its applications, which will contribute to further advances in lepidopteran and entomological research and the practical use of these insects.

Keywords: silkworm, *Bombyx mori*, transcriptome analysis, RNA-seq, gene model, transcriptional factor

Background

The silkworm *Bombyx mori* is a lepidopteran insect that has been utilized in studies of physiology, genetics, molecular biology, and pathology. Functional analyses of genes related to hormone synthesis/degradation, pheromone reception, larval marking formation, and virus resistance have been performed using this silkworm [1-5], and the findings obtained have contributed to the promotion of insect science. The silkworm has the ability to produce large amounts of silk proteins, which is one of the most prominent characteristics of this species. Silk proteins are mainly composed of the fibrous protein Fibroin and aqueous protein Sericin, which are produced in the larval tissue silk gland (SG) [6]. A transgenic technique has been applied to the silkworm [7], which has enabled the production of a large amount of recombinant proteins through the introduction of transgenes for overexpression in the SG [8]. The silkworm can be utilized as a significant bioreactor by this approach.

76 Based on its biological and industrial importance, the whole genome sequence
77 of the silkworm was reported in 2004 by two research groups [9, 10]. This was the first
78 lepidopteran genomic analysis and has served as a fundamental basis for genomic
79 studies on Lepidoptera. This silkworm genome data was updated in 2008 [11] and
80 related data have since become available, including microarray-based gene expression
81 profiles, a BAC-based linkage map, and full-length cDNA data [12-14]. These data
82 have strongly promoted studies on *B. mori* and other lepidopteran insects in the past
83 few decades.
84 A new and high-quality reference genome assembly of the silkworm p50T
85 (*daizo*) strain using PacBio long-read and Illumina short-read sequencers was reported
86 in 2019 [15]. The new genome assembly consists of 696 scaffolds with N50 of 16.8 Mb
87 and only 30 gaps. Predicted new gene model based on this novel genome assembly,
88 using cDNA, protein and RNA-seq data as hints, was constructed and was more
89 precise that the previous model made via the old genome assembly [15]. The next step
90 in the establishment of genome-related data is transcriptome data, which contains
91 reference transcriptome sequence data as well as gene expression profiles in major
92 tissues. These data will significantly contribute to advances in research on the silkworm
93 and other lepidopterans.
94 In the present study, we constructed a reference transcriptome dataset using
95 RNA-seq data obtained from ten major tissues/subparts of silkworm larvae (Fig. 1).
96 RNA-seq data were mapped on the new genome assembly and reference
97 transcriptome sequence data were successfully constructed. We also performed
98 functional annotation of the reference transcriptome using human and *Drosophila*
99 protein datasets in addition to NCBI-nr data. Established reference transcriptome
100 sequence data provided a nearly complete structure for *sericin-1* (*ser1*), a major silk
101 gene with a complex sequence. The expression of the transcriptome was investigated

102 in each tissue, and the expression of a number of transcripts was found to be confined
103 to tissues such as testis (TT). Among them, genes with transcripts that were strongly
104 expressed in the midgut (MG) formed tight genomic clusters, suggesting that they
105 originated via gene duplication. The transcripts of transcriptional factor (TF) genes
106 expressed in specific tissues or SG subparts were also detected, and we speculate
107 that these genes play key roles in the major biological process of these
108 tissues/territories. The present results will accelerate molecular biological studies on
109 the silkworm and other related species, and this is an essential milestone to promote
110 entomological research as well as the practical use of insects.
111

112 Results

113 Reference transcriptome data

114 We performed a transcriptomic analysis of major silkworm larval tissues,
115 namely, the SG, fat body (FB), MG, Malpighian tubules (MT), TT, and ovary (OV), to
116 acquire more expanded RNA-seq data (Fig. 2; Table 1). Gene expression was clearly
117 differentiated among subregions in the SG [16, 17], and, thus, we subdivided the SG
118 into five subparts and investigated gene expression in each region (the anterior silk
119 gland (ASG), anterior part of the middle silk gland (MSG_A), middle part of the middle
120 silk gland (MSG_M), posterior part of the middle silk gland (MSG_P) and posterior silk
121 gland (PSG)) (Fig. 2; Table 1). Totally ten tissues/subparts were dissected from the fifth
122 instar third day larvae of p50T strain with three biological replicates (Table 1). Thirty
123 sets of RNAs were used for RNA-seq. We mapped RNA-seq data on the reference
124 genome assembly using information from the previously established gene model [15]
125 (hereafter referred to as “gene model data (GMD)”) and constructed reference
126 transcriptome data (RTD). RTD comprises 51,926 transcripts in 24,236 loci (Fig. 3A),

127 the numbers of which are higher than those of GMD (24,236 vs 16,845 loci and 51,926
128 vs 16,880 transcripts; see Fig. 3A and 3B). Therefore, RTD is an extension of GMD. To
129 perform functional annotations, coding sequence (CDS) regions and amino acid
130 sequence data were constructed by using RTD (Additional file 1), and found that
131 39,619 transcripts, derived from 16,632 loci, had at least one CDS in RTD. The
132 predicted amino acid sequences were used for gene functional annotations by a
133 homology search against human and *Drosophila* gene sets. This analysis revealed that
134 26,698 genes showed homology to human genes and 29,177 to fruit fly genes
135 (Additional file 2). We also performed a blastp analysis using the NCBI nr database
136 and found that 43,358 amino acids had homological proteins in this database
137 (Additional file 3).
138
139 Comparison between constructed reference transcriptome data and previous gene
140 model data
141 RTD represents a marked improvement over GMD. Several misassembled genes
142 are present in GMD, as represented by KWMTBOMO00087-88, 00196-197, or 00222-
143 223 genes [15]. These genes are split into two structures even though full-length cDNA
144 data define them as single genes [14, 15]. We investigated their structures in our
145 model and found that all were accurately predicted (MSTRG.494.1, MSTRG.649.1-2,
146 and MSTRG.704.1-3) (Additional file 4: Fig. S1). The elucidated gene structure was
147 attributed to the extensive RNA-seq analysis in the present study; the previous study
148 lacked gene expression data from tissues such as TT, OV, MT, and PSG, and these
149 genes were all strongly expressed in these tissues (Additional file 5: Table S1).
150 RTD also provided a number of novel genes/isoforms. Comparisons of RTD with
151 GMD revealed that among the 51,926 transcripts identified, 7,704 belonged to the new
152 loci group, whereas 27,342 were categorized as new isoforms (Fig. 3B, see Methods).

153 Among the 7,704 new loci group transcripts, a number of genes were also present in
154 the previously established full-length cDNA-based gene model [14]. However, 2,324
155 transcripts did not hit this gene set and, thus, these genes to which these transcripts
156 belong were perceived to be novel genes. An expression analysis revealed that many
157 of these genes were commonly expressed in all of the tissues investigated herein,
158 whereas other genes were exclusively expressed in specific tissues, such as TT
159 (Additional file 6: Fig. S2). The functional annotation analysis revealed that newly
160 identified genes included a trypsin inhibitor (MSTRG.14562.2), carboxypeptidase
161 (MSTRG.16874.1-3), and pyruvate kinase (MSTRG.18651.2). Therefore, our RTD
162 represents a significant improvement over GMD (Additional file 3).
163
164 Elaborated structures of silk genes
165 Silk production is one of the most prominent characteristics of the silkworm. Silk
166 genes are strongly expressed in the silk-producing tissue SG and our extensive RNA-
167 seq data are expected to show highly elaborated models for these genes. *ser1* is one
168 of the major silk genes, is strongly expressed in the MSG, and encodes a >400-kDa
169 serine-rich protein [6, 18]. *ser1* is composed of 9 exons, among which exon 6 has a
170 long repetitive sequence with a length of ~6,500 bp [6 ,19]. The full-length sequence of
171 this exon has yet to be elucidated due to its complexity. We herein demonstrated that
172 our model MSTRG.2477.1 provided an almost complete sequence for this exon (6,234
173 bp, Additional file 7: Fig. S3). Exon 6 encodes serine, glycine, threonine, asparagine,
174 and aspartic acid-rich residues (Additional file 8: Fig. S4), which is consistent with
175 previous findings showing that Ser1 comprises large numbers of these residues
176 (Additional file 9: Table S2) [20]. The detailed structural analysis revealed that the long
177 repetitive motif identified here comprised 53 repeats of a 38-amino acid unit (Additional
178 file 10: Fig. S5). Each unit had serine-rich residues and a slight difference was

179 observed in sequences among units (Additional file 10: Fig. S5) [6]. The 38-amino acid-
180 based repeat unit was also observed in exon 8 of *ser1* (Additional file 8: Fig. S4;
181 Additional file 10: Fig. S5) or in the sericins of saturniid species [6, 21], and, thus, the
182 repeat unit of this length is expected to have a structural function in a number of sericin
183 proteins.

184 We also observed significant improvements for other *sericin* genes. Sericin-3
185 (Ser3) is another major silk protein that has a relatively soft texture and possesses
186 serine-rich residues [22, 23]. In GMD, a 73-bp deletion was detected in exon 3, and
187 due to this structural error, a frame shift was present in the predicted amino acid
188 sequence (KWMTBOMO06311; Additional file 11: Fig. S6). In contrast, our RTD
189 (MSTRG.2595.1) successfully provided an accurate gene structure (Additional file 11:
190 Fig. S6). Sericin-4 (Ser4) is another sericin protein that is composed of 34 exons [24].
191 This gene is split into three distinct structures in GMD (KWMTBOMO06324,
192 KWMTBOMO06325, and KWMTBOMO06326), whereas RTD provided an exact model
193 (MSTRG.2610.1) (Additional file 12: Fig. S7). Collectively, these results suggest that
194 our RTD provided highly defined structures, even for complex silk genes.
195

196 Estimating the abundance of the reference transcriptome in multiple tissues

197 Our extensive transcriptomic analysis provided fundamental insights into gene
198 expression profiles in multiple silkworm tissues. The expression abundance of each
199 transcript was calculated as transcripts per million (tpm) (Additional file 13) and overall
200 gene expression was compared among tissues through two independent methods, one
201 for hierarchical clustering (HC) and another for a principal component analysis (PCA).
202 To avoid the effects of low expression transcripts, we performed these analyses using
203 transcripts with tpm values > 30 in at least one sample. HC using all transcript tpm data
204 was also performed for comparisons. These analyses revealed that the biological

205 replicate samples collected herein were highly reproducible because they were derived
206 from the same tissues forming tight clusters (Fig. 4; Additional file 14: Fig. S8). In the
207 HC analysis, a single cluster was formed for the MSG_M and MSG_P in each sample
208 (Fig. 4; Additional file 14: Fig. S8B), and we speculate that this was due to highly
209 conserved gene expression between these SG territories. A correlation analysis of
210 gene expression using SG transcriptome data supported this hypothesis (Additional file
211 15: Table S3). A previous study performed RNA-seq analysis of multiple silkworm
212 larval tissues in another silkworm strain, o751 [25-27], and these RNA-seq data were
213 added to our analysis (Fig. 4; Table 1; Additional file 14: Fig. S8; these samples are
214 referred to as BN_MG, BN_FB, BN_MT, BN_SG, and BN_TT). We found that the
215 samples collected from the same tissues clearly formed clusters (Fig. 4). In the o751
216 strain, the SG was collected as a whole tissue. Although all the SG subparts (MSG_A,
217 MSG_M, MSG_P, ASG and PSG) were closely located in the HC analysis of
218 transcripts with > 30 (tpm) in at least one sample, BN_SG formed a single cluster
219 distant from those of the SG subparts (Fig. 4). Therefore, our transcriptomic data is a
220 robust platform for analyzing and comparing gene expression in multiple tissues.
221
222 Transcript abundance in each tissue and in the silk gland
223 Using the data described above, we investigated gene expression in detail in
224 each tissue. We focused on genes with a tpm value > 30, which approximately
225 accounted for the top 5% of the most strongly expressed genes (data not shown), and
226 regarded such transcripts as being expressed in each tissue. We found that 711 genes
227 were expressed in all tissues (Fig. 5), suggesting ubiquitous functions. We also
228 detected genes expressed in specific tissues (Fig. 5, Additional file 16: Table S4).
229 Among them, genes solely expressed in TT were the most abundant (1882), followed
230 by those expressed in OV (799), MT (499), and MG (440) (Fig. 5, Additional file 16:

231 Table S4). We also identified genes expressed in more than two tissues, such as TT
232 and OV (397, Fig. 5). A functional enrichment analysis (FEA) was performed on genes
233 with tissue-restricted expression, and functional clusters enriched in each tissue were
234 very diversified; for example, genes exclusively expressed in the TT were strongly
235 enriched for “cilium organization”, “Huntington’s disease”, and “cilium or flagellum-
236 dependent cell motility” (Fig. 6A) whereas “Metabolism of RNA”, “regulation of mRNA
237 metabolic process”, and “ribonucleoprotein complex biogenesis” were enriched in the
238 OV (Fig. 6B). Comparisons of gene expression levels among tissues revealed that the
239 expression levels of strongly expressed genes were very high in the ASG (Fig. 7).
240 These genes comprise fungal protease inhibitors, cuticular protein genes and others
241 (Additional file 17: Table S5). In contrast, the levels of strongly expressed genes were
242 lower in the MSG-M/MSG-P (Fig. 7; Additional file 17: Table S5). We also investigated
243 the expression profiles of genes strongly expressed in each tissue and found tissue-
244 restricted expression for these genes in the MG, FB, and MSG_A and ubiquitous
245 expression for those in the other tissues examined (Additional file 17: Table S5;
246 Additional file 18: Fig. S9). The genomic positions of tissue-enriched genes were
247 examined, and genes strongly expressed in the MG formed tight genomic clusters (Fig.
248 8; Additional file 17: Table S5). We also found clusters for strongly expressed genes in
249 other tissues (Additional file 17: Table S5; Additional file 19: Fig. S10).
250 We then investigated gene expression in the SG in more detail. Previous
251 studies revealed that a number of genes showed territory-specific expression in the SG
252 [16, 17]. However, overall gene expression in each territory remains unclear. We
253 herein demonstrated that >1000 genes were commonly expressed in all SG subparts
254 and also that a number of genes were expressed in specific territories (Fig. 9). They
255 included 351 ASG-restricted, 180 MSG_A-restricted, 99 MSG_M-restricted, 71
256 MSG_P-restricted, and 100 PSG-restricted genes, respectively (Fig. 9, Additional file

257 20: Table S6). Furthermore, we identified genes that were commonly expressed in
258 more than two territories (Fig. 9). They included genes expressed in the MSG_M and
259 MSG_P (Fig. 9), and combined with the results of HC and the correlation analysis (Fig.
260 4; Additional file 15: Table S3), we speculate that gene expression is highly conserved
261 between the MSG_M and MSG_P. This result was supported by the presence of a
262 smaller number of genes expressed solely in the MSG_M or MSG_P (Fig. 9). We also
263 found that the genes that were exclusively expressed in the ASG were more abundant
264 than in other territories, and fewer genes were commonly expressed in the ASG and
265 other subparts (Fig. 9). We speculate that this reflects the functional diversification of
266 the ASG because the numbers of genes exclusively expressed in ASG (351) and those
267 expressed in the MSG and PSG (395) were comparable, suggesting similar diversified
268 functions (Fig. 9). This may also be the case for the MSG_A based on the presence of
269 similar characteristics (Fig. 9). FEA revealed that the functional clusters enriched in
270 each SG subpart were largely diversified (Additional file 21: Fig. S11).
271
272 Expression analysis of transcriptional factor genes in the silkworm
273 A transcriptomic analysis is a powerful tool for identifying genes with low levels
274 of expression. TF genes are considered to show low expression levels even though
275 they have many important functions in developmental, physiological, and other major
276 biological processes. Therefore, an expression analysis of TF genes will contribute to a
277 more detailed understanding of the silkworm biology. Silkworm TF genes have recently
278 been catalogued [28] and we investigated their expression levels in various silkworm
279 tissues using this information. According to the low level of expression of TF genes, we
280 herein perceived TF genes with a tpm value > 5 as those expressed in each tissue.
281 This analysis revealed that a number of TF genes were exclusively expressed in the
282 OV and/or TT (Fig. 10A; Additional file 22: Table S7). These genes included

283 KWMTBOMO02002 (*traffic jam*), KWMTBOMO002212 (*mirror*), KWMTBOMO01693
284 (*vismay*), and KWMTBOMO06584 (*Sox100B*), all of which play significant roles in
285 gonad morphogenesis, oogenesis, spermatogenesis, and TT differentiation in
286 *Drosophila melanogaster* (Additional file 22: Table S7) [29-32]. We also found that
287 KWMTBOMO09369/KWMTBOMO10218, the silkworm counterparts of human GATA4,
288 were expressed in the OV, similar to that in humans (Additional file 22: Table S7) [33].
289 We speculate that these TF genes have conserved functions in a wide variety of
290 organisms, possibly in the development, differentiation, or homeostasis of reproductive
291 tissues.
292 We also investigated TF gene expression in the SG. Previous studies revealed
293 the central roles of the TF genes *forkhead* (*fkh*), *Antennapedia* (*Antp*), and *Arrowhead*
294 (*Awh*) in the regulation of silk gene expression [34-38]. Other TF genes that function in
295 the regulation of silk gene expression may also exist because silk genes are strongly
296 expressed and a number of silk genes are expressed in specific territories in the SG
297 (Fig. 9). In addition to previously identified TF genes, the expression of novel TF
298 genes, such as those belonging to the High Mobility Group (HMG), Zinc Finger (ZF),
299 Paired box (PAX), or forkhead family, was confined to the SG (Fig. 10B, Additional file
300 23: Table S8). The tpm values of these genes are shown in Additional file 23: Table
301 S8, and we identified TF genes expressed solely in the ASG or MSG_A. Genes
302 expressed in more than two subparts were also detected (Additional file 23: Table S8).
303 We confirmed their expression in an RT-PCR analysis and experimental results were
304 consistent with tpm values (Additional file 24: Fig. S12). The TF genes identified herein
305 include those with indispensable roles in the development of *D. melanogaster*; for
306 example, *Dichaete* (*D*), *gooseberry-neuro* (*gsb-n*), and *sloppy paired 2* (*slp2*) are
307 essential for embryonic segmentation [39-41], *Enhancer of split mβ-HLH* (*E*(*spl*)*mβ-*
308 *HLH*) for neurogenesis [42], and *twin of eyegone* (*toe*) for eye development [43]. We

309 consider that it is very interesting if these genes have significant roles in the regulation
310 of the silk gene expression, a function that is independent from the developmental
311 regulation, in the silkworm.
312

313 Discussion

314 In the present study, we performed RNA-seq analysis of multiple larval tissues
315 from the silkworm *B. mori*. We established RTD using a recently reported high-quality
316 reference genome assembly [15] and RNA-seq data newly obtained herein. RTD
317 showed marked improvements over GMD, most notably the establishment of a nearly
318 complete structure for *ser1* (Additional file 7: Fig. S3; Additional file 8: Fig. S4); its full
319 sequence has never been entirely elucidated due to its complexity. Our results indicate
320 that an extensive RNA-seq analysis in combination with high-quality reference genome
321 data provides highly refined gene structures, even for complex genes. The cost of
322 performing a deep sequencing analysis has recently decreased and, thus, it has
323 become affordable for every researcher to conduct not only a short-read RNA-seq
324 analysis, but also long-read genome sequencing using their own species. The present
325 results are a significant proof-of-concept that highly refined gene structures may be
326 established using the combination of these data, even for non-model organisms.
327 Furthermore, more elaborate gene structures may be constructed using the RNA-seq
328 data derived from other tissues and/or stages.
329 We herein found that a number of genes showed tissue-restricted expression in
330 the silkworm (Fig. 5). Among them, genes exclusively expressed in the TT were the
331 most abundant (Fig. 5). A previous study identified a number of TT-specific genes in
332 the silkworm [12], which is consistent with the present results. The presence of a
333 number of TT-specific genes was also demonstrated in the jewel wasp, *Nasonia*
334 *vitripennis* [44], indicating that this is a common feature in insects. Recent studies on

335 *Drosophila* revealed that newly emerging genes were strongly biased for expression in
336 the male reproductive system [45]. Therefore, the TT-specific genes identified in the
337 present study may have similar traits. This issue may be confirmed by investigating the
338 evolutionary ages of these genes, and, if this is the case, addressing the question of
339 why the TT is a tissue that is permissive for new gene birth, a phenomenon observed
340 not only in insects, but also in vertebrates [46], which will become possible using the
341 silkworm. Another important result obtained from our cross-tissue gene expression
342 analysis is that genes strongly expressed in the MG showed strong tissue-restricted
343 expression and also formed tight genomic clusters (Fig. 8; Additional file 17: Table S5;
344 Additional file 18: Fig. S9). Comparisons of the sequences of these genes revealed
345 that genes in each cluster encoded homological proteins; chr.7 genes encoded
346 trypsins, chr.15 juvenile hormone-binding proteins (JHBPs), chr.16 fatty acid-binding
347 proteins, chr.19 actin cytoskeleton-regulatory complex proteins, and chr.20 multiprotein
348 bridging factor 2 (MBF2) (Additional file 17: Table S5). Among these genes, strong
349 expression in the MG has already been demonstrated for *jhbp*s [47], and Trypsin
350 proteins were present in digestive juices [48]. Homological genes that cluster in the
351 genome are generally considered to have originated via tandem gene duplication, and
352 to the best of our knowledge, few studies have investigated clustered genes that are
353 expressed in the MG. In one case study on *Drosophila*, neutral lipase genes expressed
354 in the MG clustered in the genome and were presumably under positive selection to
355 retain different substrate specificities towards new lipid components of the diet [49].
356 Based on these findings, the genes identified in the present study may also have
357 advantages in the silkworm MG, such as enhancing activity for digestion and/or
358 xenobiotic detoxification. The present study provides valuable insights into gene
359 evolution as well as neofunctionalization in insects, which may be validated in more
360 detail in future studies. In addition, the results obtained herein will facilitate the practical

361 application of the silkworm; targeted gene integration into the clusters identified in the
362 present study will enable strong gene expression in the MG, which will contribute to the
363 establishment of strains with valuable properties, such as increased antiviral or
364 antibiotic activities. The latest genome editing technologies should promote the
365 establishment of useful silkworm strains.

366 Our detailed gene expression analysis provides fundamental information on the
367 traits of the SG, particularly each subpart. The SG is a tissue that arises from a single
368 embryonic segment and has a long tubular structure [50]. Gene expression in each SG
369 subpart is largely diversified, as demonstrated herein (Fig. 9; Additional file 20: Table
370 S6) and in previous studies [16, 17]. The most important result of the present study is
371 that overall gene expression in the ASG was diversified the most within the SG, as
372 demonstrated by the presence of a number of genes exclusively expressed in the ASG
373 (351, Fig. 9), a number of genes expressed both in the MSG and PSG (395, Fig. 9),
374 and the location of the ASG at the outermost site in the SG cluster in the HC analysis
375 (Fig. 4). We speculate that these results indicate the functional diversification of the
376 ASG, which is consistent with previous findings showing that the ASG functions in silk
377 fiber processing and the MSG/PSG in silk protein production [51]. FEA revealed that
378 functional clusters enriched in the ASG were “carbohydrate metabolic process” and
379 “Transport of small molecules” (Additional file 21: Fig. S11A), while those enriched in
380 the MSG/PSG were “ribonucleoprotein complex biogenesis” and “Translation”
381 (Additional file 21: Fig. S11F), further supporting this concept. In this context, another
382 result showing that gene expression in the MSG_A also showed diversification is of
383 interest. We demonstrated that genes specifically expressed in the MSG_A were
384 abundant (180, Fig. 9), a number of genes were commonly expressed in the
385 MSG_M/MSG_P/PSG (335, Fig. 9), and the MSG_A was located at the outermost site
386 in the MSG/PSG cluster in the HC analysis (Fig. 4). MSG_A is a part of the MSG and

387 functions in the production of the sericin proteins Ser2 and Ser3 [23, 52], similar to the
388 function of the MSG_M/MSG_P in the production of Ser1 [20]. Nevertheless, our
389 results indicate that gene expression in the MSG_A was more diverse than that in the
390 MSG_M/MSG_P compared with that of the PSG; the PSG is the territory that produces
391 fibroin and not sericin [53], whereas gene expression appeared to be more conserved
392 between the PSG and MSG_M/MSG_P than between the MSG_A and
393 MSG_M/MSG_P (Figs. 4 and 9). These results may be attributed to the presence of a
394 number of genes that are strongly and specifically expressed in the MSG_A, including
395 ecdysone oxidase, fatty acid hydroperoxide dehydratase, and other genes (Fig. 9;
396 Additional file 20: Table S6). We found that genes strongly expressed in the MSG_A
397 were enriched for the functional clusters of “Metabolism of vitamins and cofactors” and
398 “organic hydroxy compound transport” (Additional file 21: Fig. S11B), and speculated
399 that these clusters define the biological functions that are unique to this territory.
400 Therefore, our extensive RNA-seq analysis provides fundamental insights into the
401 functions of the SG as well as its evolution, which has not yet been elucidated in detail.
402 In the Lepidoptera, the morphology of the SG is largely diversified among species [54]
403 and the Saturniidae, a family that is phylogenetically close to the Bombycidae, have
404 MSGs with one territory and no morphological separation [6]. Therefore, the
405 differentiation of MSG gene expression observed herein may be specific to *B. mori*
406 and/or other closely related species. Further studies are needed to clarify whether
407 differences in gene expression among species are a driving force that generates
408 diversity in cocoon properties, including shape, size, and physical activity. The TF
409 genes identified in the present study may be one of the key factors responsible for the
410 differences in gene expression within the SG or among species.
411 In the present study, we established RTD for the silkworm and performed a
412 detailed examination of gene expression in silkworm tissues. The results obtained will

413 contribute to our understanding of silkworm biology and further promote the industrial
414 application of the silkworm and other insects.
415

416 Conclusions

417 We performed RNA-seq analysis of the major larval tissues of the silkworm and
418 established RTD. Using these data, we successfully improved the gene structure and
419 clarified gene expression in detail in each tissue. The present results are a
420 fundamental basis for the further promotion of silkworm research and will contribute to
421 the practical application of insects.
422

423 Methods

424 Silkworm rearing, RNA extraction, and sequencing

425 The silkworm p50T strain was reared on an artificial diet (Nihon Nosan Kogyo,
426 Yokohama, Japan) at 25°C under a 12-hour light/dark photoperiod. The SG, FB, MG,
427 MT, TT, and OV were dissected on the third day of the fifth instar larvae. The SG was
428 further subdivided into the ASG, MSG_A, MSG_M, MSG_P, and PSG. Each
429 tissue/subpart was dissected from one individual, and three biological replicates were
430 obtained and separately analyzed (see Table 1). Tissues were homogenized using
431 ISOGEN (NIPPON GENE, Tokyo, Japan) and the SV Total RNA Isolation System
432 (Promega, Madison, WI) was used for RNA extraction. The total RNA samples
433 extracted were sequenced by Illumina NovaSeq6000 (Macrogen Japan Corp., Kyoto,
434 Japan).
435

436 Construction of RTD and estimation of the expression of each transcript

437 The raw RNA-seq data of 30 samples were trimmed by Trimmomatic version
438 0.36 [55]. The trimmed RNA-seq data of each tissue were mapped to the new
439 reference genome with a new gene model [15] by HISAT2 version 2.1.0 [56]. Mapped
440 data were each assembled to transcriptome data by StringTie version 1.3.3 [57]. The
441 30 transcriptome datasets were merged into one transcriptome dataset, referred to as
442 “a reference transcriptome” by StringTie. GffCompare version 0.10.6 was used [58] for
443 comparisons with the reference transcriptome and previously reported gene sets [15].
444 The transcripts detected at the newly identified loci were categorized into the “New loci”
445 group, those newly detected at the previously identified loci into the “New isoform”
446 group, and other genes and transcripts into “Identified in gene models” (see Fig. 3B).
447 To estimate the expression of the reference transcriptome in 30 samples, the
448 raw fastq data of each sample and reference transcript data were used with Kallisto
449 version 0.44.0 [59]. The raw RNA-seq data of multiple tissues in *B. mori* strain o751
450 from the Sequence Read Archive (SRA) and reference transcript data were used in
451 comparisons of transcriptome data: the accession numbers of raw RNA-seq data are
452 DRA005094, DRA005878, and DRA005094 [25-27].
453 We used TIBCO Spotfire Desktop (version 7.6.0) software with the “Better
454 World” program license (TIBCO, Inc., Palo Alto, CA; [60]) for the classification of
455 differentially expressed samples in silkworm tissues in HC using Ward’s method.
456 Morpheus was also used [61] for HC. R (version 3.6.0) was used in the PCA analysis
457 [62]. Regarding Venn diagram construction and the scatter plot analysis, R (version
458 4.0.2) was used [63]. The relationships among gene expression profiles in the SG
459 territories were evaluated using Spearman’s rank correlation.
460
461 <u>Annotation for the reference transcriptome and FEA</u>

462 Transcoder (version 5.5.0) was used to identify coding regions within transcript
463 sequences and convert transcript sequences to amino acid sequences
464 [64]. Transcriptome sequence sets were compared at the predicted amino acid
465 sequence level by the successive execution of the blastp program in the NCBI BLAST
466 software package (version 2.9.0+) with default parameters and an e-value cut-off of 1e-
467 10 [65]. Regarding the reference database sets to be blasted, human and fruit fly (*D.*
468 *melanogaster*) protein datasets in the Ensembl database (v.97) were used because the
469 sequences of these organisms were functionally well-annotated and amenable to
470 computational methods, such as a pathway analysis [66]. The names of the top-hit
471 genes in the human and fruit fly datasets were annotated to *B. mori* transcripts utilizing
472 Ensembl Biomart [67] and Spotfire Desktop software under TIBCO Spotfire's "Better
473 World" program license (TIBCO Software, Inc., Palo Alto, CA, USA) [60]. Functional
474 enrichment analyses were performed using the metascape portal site [68]
475 with annotation results against the human gene set.
476
477 Comparison of gene structures among different models
478 Gene structures among RTD, GMD, and cDNA-based data were compared in the
479 silkbase [69] or KAIKObase [70]. Amino acid sequences were aligned using CLC
480 Genomics Workbench 20.0.04 (QIAGEN, Aarhus, Denmark).
481
482 RT-PCR
483 cDNA was synthesized using Superscript IV (Thermo Fisher Scientific Inc., Waltham,
484 MA, USA) according to the manufacturer's instructions. Five hundred nanograms of
485 total RNAs extracted from the ASG, MSG_A, MSG_M, MSG_P, and PSG were used
486 for the cDNA synthesis. KOD FX neo polymerase (Toyobo, Osaka, Japan) was used
487 for RT-PCR. PCR conditions were as follows: 95°C for 1 min followed by 22 cycles (for

488 *rp49*) or 30 cycles (for TF genes) of 95°C for 30 sec, 58°C for 30 sec, followed by 68°C
489 for 1 min, and additional 68 °C for 1 min after the cyclic phase. Primer sequences are
490 listed in Additional file 25: Table S9.

491 Declarations

492 **Availability of data and materials**

493 The RNA-seq reads supporting the conclusions of the present study are available in
494 the SRA with accession number DRA008737 (The accession number of RNA-seq data
495 of each sample is shown in Table 1).
496 Reference transcriptome data is available at the Transcriptome Shotgun Assembly
497 (TSA) database under accession IDs ICPK01000001-ICPK01051926, and the Gff file
498 of the transcriptome was available via DOI: 10.18908/lsdba.nbdc02443-001.V001.
499 The estimated abundance of transcripts is available from the Gene Expression Archive
500 (GEA) in DDBJ under accession ID E-GEAD-315 or from The Life Science Database
501 Archive (DOI: 10.18908/lsdba.nbdc02443-002.V001).
502 Additional data are available in The Life Science Database Archive (the title in the
503 Archive is "KAIKO - Metadata of reference transcriptome data"
504 (DOI:10.18908/lsdba.nbdc02443-000.V001)) and figshare (DOI:
505 10.6084/m9.figshare.c.5333894).
506 Additional file 1
507 Predicted amino acid sequences of reference transcriptome.
508 DOI:10.18908/lsdba.nbdc02443-004
509 Additional file 2
510 Functional annotations of the reference transcriptome (blast against human and
511 *Drosophila* gene sets). DOI:10.18908/lsdba.nbdc02443-003
512 Additional file 3

513 Functional annotations of the reference transcriptome (blast against the NCBI nr
514 database). DOI:10.6084/m9.figshare.14192741.
515 Additional file 4: Fig. S1
516 Comparison of gene structures among gene model data, cDNA-based data, and
517 reference transcriptomic data. (A) Locus around KWMTBOMO00087, (B)
518 KWMTBOMO00196, and (C) KWMTBOMO00222. GMD; gene model data, CBD;
519 cDNA-based data, RTD; reference transcriptomic data.
520 DOI:10.6084/m9.figshare.14205785
521 Additional file 5: Table S1
522 Tpm values in MSTRG.494.1, MSTRG.649.1-2 and MSTRG.704.1-3. DOI:
523 10.6084/m9.figshare.14206034
524 Additional file 6: Fig. S2
525 Expression of new loci transcripts that did not hit the cDNA-based gene model.
526 Numbers indicate transcripts with a tpm value >0.01 in each tissue. SG, silk gland
527 (using average tpm values in the five SG subparts); FB, fat body; MG, mid gut; MT,
528 Malpighian tubules; OV, ovary; TT, testis. DOI: 10.6084/m9.figshare.14217335
529 Additional file 7: Fig. S3
530 Structure of the *sericin-1* gene. MSTRG.2477.1 has a long exon 6.GMD; gene model
531 data, CBD; cDNA-based data, RTD; reference transcriptomic data. DOI:
532 10.6084/m9.figshare.14206166
533 Additional file 8: Fig. S4
534 The presumptive full-length amino acid sequence of sericin-1 deduced by reference
535 transcriptomic data (MSTRG.2477.1). The orange characters show the amino acids
536 encoded by exon 6 and blue characters by exon 8. DOI:
537 10.6084/m9.figshare.14206736
538 Additional file 9: Table S2

539 Comparisons of the sericin-1 amino acid composition elucidated by an amino acid
540 analysis and gene model. Mole% is shown. DOI: 10.6084/m9.figshare.14206748
541 Additional file 10: Fig. S5
542 Sequence of the 38-amino acid-based repeat unit encoded by exon 6 and exon 8 in
543 sericin-1. Exon 6 comprises 53 repeats and exon 8 13 repeats. DOI:
544 10.6084/m9.figshare.14212673
545 Additional file 11: Fig. S6
546 Comparison of the sericin-3 sequence among different gene models. The amino acid
547 sequences identified in the previous study (NM_001114644; [23]), derived from cDNA-
548 based data (BMgn014348), reference transcriptomic data (MSTRG.2595.1), and gene
549 model data (KWMTBOMO06311), are shown. Amino acids that differ in
550 KWMTBOMO06311 are shown as white letters. Note that a frame shift occurs in the
551 gene model data. DOI: 10.6084/m9.figshare.14216927
552 Additional file 12: Fig. S7
553 Comparison of the *sericin-4* gene structure. The gene structures elucidated by the
554 previous study (*sericin-4*; [24]) and modeled by gene model data (GMD) and reference
555 transcriptomic data (RTD) are shown. DOI: 10.6084/m9.figshare.14216951
556 Additional file 13
557 Expression data of each transcript in multiple tissues. DOI: 10.18908/lsdba.nbdc02443-
558 002.V001
559 Additional file 14: Fig. S8
560 (A) Principal Component Analysis (PCA) results with expression profiles in 45 samples
561 of transcripts showing a tpm value > 30 in at least one sample. Abbreviations and the
562 numbers of samples are the same as in Fig. 4. The X axis and Y axis are principal
563 components 1 (PC1) and PC2, respectively. (B) Hierarchical clustering of expression

564 data in 45 samples using all transcript tpm values. DOI:
565 10.6084/m9.figshare.14216993.
566 Additional file 15: Table S3
567 Spearman's rank correlation coefficient among silk gland territories. DOI:
568 10.6084/m9.figshare.14217071
569 Additional file 16: Table S4
570 List of genes expressed in specific tissues. DOI: 10.6084/m9.figshare.14217206
571 Additional file 17: Table S5
572 List of genes strongly expressed in each tissue or in silk gland subparts. The top 50
573 strongly expressed genes are shown. DOI: 10.6084/m9.figshare.14217218
574 Additional file 18: Fig. S9
575 A scatter plot of gene expression in each tissue. Each spot shows the tpm value. The
576 top ten ranked strongly expressed genes in (A) ASG, (B) MSG_A, (C) MSG_M, (D)
577 MSG_P, (E) PSG, (F) FB, (G) MG, (H) MT, (I) OV and (J) TT are marked in red. DOI:
578 10.6084/m9.figshare.14217227
579 Additional file 19: Fig. S10
580 Genomic position of genes strongly expressed in each tissue. In (A), genes strongly
581 expressed in the ASG only are shown with a red bar, in subparts other than the ASG
582 with a green bar, and those commonly expressed in the ASG and other tissues with a
583 yellow bar. This same applies to MSG_A (B), MSG_M (C), MSG_P (D), PSG (E), FB
584 (F), MT (G), OV (T), and TT (I). (A') shows the chr. 11 of the ASG and (F') shows chr.
585 20 of the FB. Regarding the MG, see Fig. 8. The top 50 strongly expressed genes are
586 shown. The black bar indicates the chromosome, and the number at the left side of
587 each chromosome indicates the chromosomal number. DOI:
588 10.6084/m9.figshare.14217233
589 Additional file 20: Table S6

List of territory-specific genes in the silk gland. DOI: 0.6084/m9.figshare.14217242

Additional file 21: Fig. S11

Results of the enrichment analysis for territory-specific transcripts in the silk gland. The number of transcripts used for the analysis is shown in the bracket. -log10 (P) represents -log10 (P-value). For example, -log10 (P)=5 represents P-value= 10^{-5}. DOI: 10.6084/m9.figshare.14217257

Additional file 22: Table S7

List of tissue-specific TF genes. DOI: 10.6084/m9.figshare.14217272

Additional file 23: Table S8

List of territory-specific TF genes in the silk gland. DOI: 10.6084/m9.figshare.14217296

Additional file 24: Fig. S12

RT-PCR of TF genes showing territory-specific expression in the SG. DOI: 10.6084/m9.figshare.14217299

Additional file 25: Table S9

Primer sequences used for RT-PCR. DOI: 10.6084/m9.figshare.14217308

Competing interests

The authors declare no conflicts of interest.

Funding

This work was supported by the National Bioscience Database Center of the Japan Science and Technology Agency (JST) to HB.

This work was supported by the Cabinet Office, Government of Japan, Cross-ministerial Strategic Innovation Promotion Program (SIP), “Technologies for Smart Bio-industry and Agriculture” (funding agency: Bio-oriented Technology Research Advancement Institution, NARO) to KY, TT, and HS.

This work was also supported by a grant from the Ministry of Agriculture, Forestry and Fisheries of Japan (Research Project for Sericultural Revolution) to KY, TT, and HS.

Author contributions

Conceived and designed experiments: KY, TT, and HS.

Performed experiments: TT.

Contributed reagents/materials/analysis tools: HS.

Analyzed data: KY, TT, AJ, and HB.

Contributed to the writing of the manuscript under the draft version: KY, TT, and HB.

All authors discussed the data and helped with manuscript preparation. KY supervised the project.

All authors read and approved the final manuscript.

Acknowledgments

The computing resource was partly provided by the super computer system at the National Institute of Genetics (NIG), Research Organization of Information and Systems (ROIS), Japan. The authors thank Mrs. Kaoru Nakamura and Toshihiko Misawa for rearing the silkworms, Ms. Satoko Kawamoto for technical assistance, and Dr. Jianqiang Sun for data analysis advice.

Legends

Fig. 1. Workflow of the data analysis performed in the present study. To obtain reference transcriptome sequences, Fastq data of 10 tissues/subparts from 5th instar larvae were mapped to the new reference genome [15]. Kallisto software was used to

641 estimate the expression abundance of each transcript in these tissues. Regarding
642 RNA-seq data obtained from the public database (o751 strain), see Table 1. We
643 performed a Blast search against human and *Drosophila* genome data to perform
644 functional annotations of the reference transcriptome. Insect, human, database
645 images, and sequencer drawings [71] are licensed at Creative Commons [72].
646
647 Fig. 2. (A) Final (5th) instar larva of the silkworm p50T (*daizo*) strain. Scale bar = 5 mm.
648 (B, C) Male (B) or (C) female individuals dissected on the third day of fifth instar larvae.
649 Scale bar = 5 mm. MG, mid gut; TT, testis; MT, Malpighian tubules; SG, silk gland; FB,
650 fat body; OV, ovary. (D, D') Image (D) and schematic (D') of the silk gland. ASG,
651 anterior silk gland; MSG_A, anterior part of the middle silk gland; MSG_M, middle part
652 of the middle silk gland; MSG_P, posterior part of the middle silk gland; PSG, posterior
653 silk gland. Scale bar = 2.5 mm.
654
655 Fig. 3. Basal characteristics of the reference transcriptome. (A) Comparison of gene
656 model data [15] and the reference transcriptome data of the present study. The
657 numbers of loci and transcripts are shown. These numbers were calculated from gff
658 files of the two data sets. (B) Classification of 51,926 transcripts. Each transcript was
659 classified into three categories, and the numbers of the three categories are shown in a
660 pie chart. Definitions of the three categories are described in the main text.
661
662 Fig. 4. Hierarchical clustering of expression data in 45 samples of transcripts showing a
663 tpm value > 30 in at least one sample. Abbreviations that start with "BN" indicate
664 samples collected in the previous study [25-27]. The numbers added to the
665 abbreviations mean biological replicates.
666

667 Fig. 5. Venn diagram showing transcripts expressed in each tissue. The number of
668 transcripts with a tpm value >30 is shown. SG, silk gland; FB, fat body; MG, mid gut;
669 MT, Malpighian tubules; OV, ovary; TT, testis.
670
671 Fig. 6. Results of the enrichment analysis by Metascape in testis (TT) (A) and ovary
672 (OV) (B). An enrichment analysis was performed using annotation data against the
673 human gene set of the reference transcripts expressed in specific tissues. -log10 (P)
674 represents -log10 (P-value). For example, -log10 (P)=5 represents P-value= 10^{-5}.
675
676 Fig. 7. A scatter plot of gene expression in each tissue. Each spot shows the tpm
677 value.
678
679 Fig. 8. Genomic position of genes strongly expressed in the MG only (red bar), in other
680 than the MG (green bar), and commonly in the MG and other tissues (yellow bar). The
681 top 50 strongly expressed genes are shown. The black bar indicates the chromosome.
682 The number at the left side of each chromosome indicates the chromosomal number.
683 (A) Genomic positions of all chromosomes. (B) Genomic positions of chromosomes 7,
684 15, 16, 19 and 20, in which the tight clusters of strongly expressed genes in the MG
685 are present.
686
687 Fig. 9. Venn diagram showing the number of transcripts with a tpm value >30 in each
688 silk gland part.
689
690 Fig. 10. Venn diagrams showing the number of TF genes with a tpm value >5 in each
691 tissue (A) and in silk gland subparts (B).
692

693 # References

694 1. Tan A, Tanaka H, Tamura T, Shiotsuki T. Precocious metamorphosis in transgenic
695 silkworms overexpressing juvenile hormone esterase. Proc Natl Acad Sci U S A.
696 2005; doi:10.1073/pnas.0500954102.
697 2. Ito K, Kidokoro K, Sezutsu H, Nohata J, Yamamoto K, Kobayashi I, et al. Deletion
698 of a gene encoding an amino acid transporter in the midgut membrane causes
699 resistance to a *Bombyx* parvo-like virus. Proc Natl Acad Sci U S A. 2008;
700 doi:10.1073/pnas.0711841105.
701 3. Sakurai T, Mitsuno H, Haupt SS, Uchino K, Yokohari F, Nishioka T, et al. A single
702 sex pheromone receptor determines chemical response specificity of sexual
703 behavior in the silkmoth *Bombyx mori*. PLoS Genet. 2011;
704 doi:10.1371/journal.pgen.1002115.
705 4. Daimon T, Uchibori M, Nakao H, Sezutsu H, Shinoda T. Knockout silkworms reveal
706 a dispensable role for juvenile hormones in holometabolous life cycle. Proc Natl
707 Acad Sci U S A. 2015; doi:10.1073/pnas.1506645112.
708 5. Kondo Y, Yoda S, Mizoguchi T, Ando T, Yamaguchi J, Yamamoto K, et al. Toll
709 ligand Spätzle3 controls melanization in the stripe pattern formation in caterpillars.
710 Proc Natl Acad Sci U S A. 2017; doi:10.1073/pnas.1707896114.
711 6. Yukuhiro K, Sezutsu H, Tsubota T, Takasu Y, Kameda T, Yonemura Y. Insect silks
712 and cocoons: structural and molecular aspects. In: Cohen E, Moussian B, editors.
713 Extracellular composite matrices in Arthropods. Cham: Springer; 2016;
714 doi:10.1007/978-3-319-40740-1_18.
715 7. Tamura T, Thibert C, Royer C, Kanda T, Abraham E, Kabma B, et al. Germline
716 transformation of the silkworm *Bombyx mori* L. using a *piggyBac* transposon-
717 derived vector. Nat Biotechnol. 2000; doi:10.1038/71978.

718 8. Tatematsu K, Kobayashi I, Uchino K, Suzutsu H, Iizuka T, Yonemura N, et al.
719 Construction of a binary transgenic gene expression system for recombinant
720 protein production in the middle silk gland of the silkworm *Bombyx mori*. Transgenic
721 Res. 2010; doi:10.1007/s11248-009-9328-2.
722 9. Mita K, Kasahara M, Sasaki S, Nagayasu Y, Yamama T, Kanamori H, et al. The
723 genome sequence of silkworm, *Bombyx mori*. DNA Res. 2004;
724 doi:10.1093/dnares/11.1.27.
725 10. Xia Q, Zhou Z, Lu C, Cheng D, Dai F, Li B, et al. A draft sequence for the genome
726 of the domesticated silkworm (*Bombyx mori*). Science. 2004;
727 doi:10.1126/science.1102210.
728 11. The International Silkworm Genome Consortium. The genome of a lepidopteran
729 model insect, the silkworm *Bombyx mori*. Insect Biochem Mol Biol. 2008;
730 doi:10.1016/j.ibmb.2008.11.004.
731 12. Xia Q, Cheng D, Duan J, Wang G, Cheng T, Zha X, et al. Microarray-based gene
732 expression profiles in multiple tissues of the domesticated silkworm, *Bombyx mori*.
733 Genome Biol. 2007; doi:10.1186/gb-2007-8-8-r162.
734 13. Yamamoto K, Nohata J, Kadono-Okuda K, Narukawa J, Sasanuma M, Sasanuma
735 S, et al. A BAC-based integrated linkage map of the silkworm *Bombyx mori*.
736 Genome Biol. 2008; doi:10.1186/gb-2008-9-1-r21.
737 14. Suetsugu Y, Futahashi R, Kanamori H, Kadono-Okuda K, Sasanuma S, Narukawa
738 J, et al. Large scale full-Length cDNA sequencing reveals a unique genomic
739 landscape in a lepidopteran model insect, *Bombyx mori*. G3. 2013;
740 doi:10.1534/g3.113.006239.
741 15. Kawamoto M, Jouraku A, Toyoda A, Yokoi K, Minakuchi Y, Katsuma S, et al. High-
742 quality genome assembly of the silkworm, *Bombyx mori*. Insect Biochem Mol Biol.
743 2019; doi:10.1016/j.ibmb.2019.02.002.

744 16. Chang H, Cheng T, Wu Y, Hu W, Long R, Liu C, et al. Transcriptomic analysis of
745 the anterior silk gland in the domestic silkworm (*Bombyx mori*) – insight into the
746 mechanism of silk formation and spinning. PLoS One. 2015;
747 doi:10.1371/journal.pone.0139424.
748 17. Shi R, Ma S, He T, Peng J, Zhang T, Chen X, et al. Deep insight into the
749 transcriptome of the single silk gland of *Bombyx mori*. Int J Mol Sciences. 2019;
750 doi:10.3390/ijms20102491.
751 18. Ishikawa E, Suzuki Y. Tissue- and stage-specific expression of sericin genes in the
752 middle silk gland of *Bombyx mori*. Dev Growth Differ. 1985; doi:10.1111/j.1440-
753 169X.1985.00073.x.
754 19. Garel A, Deleage G, Prudhomme J-C. Structure and organization of the *Bombyx*
755 *mori* Sericin 1 gene and of the Sericins 1 deduced from the sequence of the Ser 1B
756 cDNA. Insect Biochem Mol Biol. 1997; doi:10.1016/s0965-1748(97)00022-2.
757 20. Takasu Y, Yamada H, Tsubouchi K. Isolation of three main sericin components
758 from the cocoon of the silkworm, *Bombyx mori*. Biosci Biotechnol Biochem. 2002;
759 doi:10.1271/bbb.66.2715.
760 21. Zurovec M, Yonemura N, Kludkiewicz B, Sehnal F, Kodrik D, Viera LC, et al.
761 Sericin composition in the silk of *Antheraea yamamai*. Biomacromolecules. 2016;
762 doi:10.1021/acs.biomac.6b00189.
763 22. Takasu Y, Yamada H, Tsubouchi K. The silk sericin component with low
764 crystallinity. Sanshi-Konchu Biotec. 2006; doi:10.11416/konchubiotec.75.133.
765 23. Takasu Y, Yamada H, Tamura T, Sezutsu H, Mita K, Tsubouchi K. Identification
766 and characterization of a novel sericin gene expressed in the anterior middle silk
767 gland of the silkworm *Bombyx mori*. Insect Biochem Mol Biol. 2007;
768 doi:10.1016/j.ibmb.2007.07.009.

769 24. Dong Z, Guo K, Zhang X, Zhang T, Zhang Y, Ma S. Identification of *Bombyx mori*
770 sericin 4 protein as a new biological adhesive. Int J Biol Macromol. 2019;
771 doi:10.1016/j.ijbiomac.2019.03.166.
772 25. Kikuchi A, Nakazato T, Ito K, Nojima Y, Yokoyama T, Iwabuchi K, et al.
773 Identification of functional enolase genes of the silkworm *Bombyx mori* from public
774 databases with a combination of dry and wet bench processes. BMC Genomics.
775 2017; doi:10.1186/s12864-016-3455-y.
776 26. Ichino F, Bono H, Nakazato T, Toyoda A, Fujiyama A, Iwabuchi K, et al.
777 Construction of a simple evaluation system for the intestinal absorption of an orally
778 administered medicine using *Bombyx mori* larvae. Drug Discov Ther. 2018;
779 doi:10.5582/ddt.2018.01004.
780 27. Kobayashi Y, Nojima Y, Sakamoto T, Iwabuchi K, Nakazato T, Bono H, et al.
781 Comparative analysis of seven types of superoxide dismutases for their ability to
782 respond to oxidative stress in *Bombyx mori*. Sci Rep. 2019; doi:10.1038/s41598-
783 018-38384-8.
784 28. Zhu Z, Guan Z, Liu G, Wang Y, Zhang Z. SGID: a comprehensive and interactive
785 database of the silkworm. Database. 2019; doi:10.1093/database/baz134.
786 29. Zhao D, Woolner S, Bownes M. The Mirror transcription factor links signaling
787 pathways in *Drosophila* oogenesis. Dev Genes Evol. 2000;
788 doi:10.1007/s004270000081.
789 30. Li MA, Alls JD, Avancini RM, Koo K, Godt D. The large Maf factor Traffic Jam
790 controls gonad morphogenesis in *Drosophila*. Nat Cell Biol. 2003;
791 doi:10.1038/ncb1058.
792 31. Wang Z, Mann RS. Requirement for two nearly identical TGIF-related homeobox
793 genes in *Drosophila* spermatogenesis. Development. 2003; doi:10.1242/dev.00510.

794 32. Nanda S, DeFalco TJ, Loh SHY, Phochanukul N, Camara N, Doren MV, et al.
795 *Sox100B*, a *Drosophila* group E Sox-domain gene, is required for somatic testis
796 differentiation. Sex Dev. 2009; doi: 10.1159/000200079.
797 33. Vaskivuo TE, Anttonen M, Herva R, Billig H, Dorland M, Velde ERT, et al. Survival
798 of human ovarian follicles from fetal to adult life: apoptosis, apoptosis-related
799 proteins, and transcription factor GATA-4. J Clin Endocrinol Metab. 2001;
800 doi:10.1210/jcem.86.7.7679.
801 34. Mach V, Takiya S, Ohno K, Handa H, Imai T, Suzuki Y. Silk gland factor-1 involved
802 in the regulation of *Bombyx* sericin-1 gene contains fork head motif. J Biol Chem.
803 1995; doi:10.1074/jbc.270.16.9340.
804 35. Ohno K, Sawada J, Takiya S, Kimoto M, Matsumoto A, Tsubota T, et al. Silk gland
805 factor-2, involved in fibroin gene transcription, consists of LIM homeodomain, LIM-
806 interacting, and single-stranded DNA-binding proteins. J Biol Chem. 2013;
807 doi:10.1074/jbc.M113.514471.
808 36. Kimoto M, Tsubota T, Uchino K, Sezutsu H, Takiya S. Hox transcription factor Antp
809 regulates *sericin-1* gene expression in the terminal differentiated silk gland of
810 *Bombyx mori*. Dev Biol. 2014; doi:10.1016/j.ydbio.2013.12.002.
811 37. Kimoto M, Tsubota T, Uchino K, Sezutsu H, Takiya S. LIM-homeodomain
812 transcription factor Awh is a key component activating all three fibroin genes, *fibH*,
813 *fibL* and *fhx*, in the silk gland of the silkworm, *Bombyx mori*. Insect Biochem. Mol.
814 Biol. 2015; doi:10.1016/j.ibmb.2014.11.003.
815 38. Tsubota T, Tomita T, Uchino K, Kimoto M, Takiya S, Kajiwara H, et al. A *Hox* gene,
816 *Antennapedia*, regulates expression of multiple major silk protein genes in the
817 silkworm *Bombyx mori*. J Biol Chem. 2016; doi:10.1074/jbc.M115.699819.

818 39. Baumgartner S, Bopp D, Burri M, Noll M. Structure of two genes at the *gooseberry*
819 locus related to the *paired* gene and their spatial expression during *Drosophila*
820 embryogenesis. Genes Dev. 1987; doi:10.1101/gad.1.10.1247.
821 40. Grossniklaus U, Pearson RK, Gehring WJ. The *Drosophila sloppy paired* locus
822 encodes two proteins involved in segmentation that show homology to mammalian
823 transcription factors. Genes Dev. 1992; doi:10.1101/gad.6.6.1030.
824 41. Russell SRH, Sanchez-Soriano N, Wright CR, Ashburner M. The *Dichaete* gene of
825 *Drosophila melanogaster* encodes a SOX-domain protein required for embryonic
826 segmentation. Development. 1996;122:3669-76.
827 42. Couturier L, Mazouni K, Corson F, Schweisguth F. Regulation of Notch output
828 dynamics via specific E(spl)-HLH factors during bristle patterning in *Drosophila*. Nat
829 Commun. 2019; doi:10.1038/s41467-019-11477-2.
830 43. Yao J-G, Weasner BM, Wang L-H, Jang C-C, Weasner B, Tang C-Y, et al.
831 Differential requirements for the Pax6(5a) genes *eyegone* and *twin of eyegone*
832 during eye development in Drosophila. Dev Biol. 2008;
833 doi:10.1016/j.ydbio.2007.12.037.
834 44. Ferree PM, Fang C, Mastrodimos M, Hay BA, Amrhein H, Akbari OS. Identification
835 of genes uniquely expressed in the germ-line tissues of the jewel wasp *Nasonia*
836 *vitripennis*. G3(Bethesda). 2015; doi:10.1534/g3.115.021386.
837 45. Kondo S, Vedanayagam J, Mohammed J, Eizadshnass S, Kan L, Pang N, et al.
838 New genes often acquire male-specific functions but rarely become essential in
839 *Drosophila*. Genes Dev. 2017; doi:10.1101/gad.303131.117.
840 46. Kaessmann H. Origins, evolution, and phenotypic impact of new genes. Genome
841 Res. 2010; doi:10.1101/gr.101386.109.

842 47. Li W, Cheng T, Hu W, Peng Z, Liu C, Xia Q. Genome-wide identification and
843 analysis of JHBP-domain family members in the silkworm *Bombyx mori*. Mol Genet
844 Genomics. 2016; doi:10.1007/s00438-016-1245-5.
845 48. Hu X, Zhu M, Wang S, Zhu L, Xue R, Cao G, et al. Proteomics analysis of digestive
846 juice from silkworm during *Bombyx mori* nucleopolyhedrovirus infection.
847 Proteomics. 2015, doi:10.1002/pmics.201400475.
848 49. Horne I, Haritos, VS. Multiple tandem gene duplications is a neural lipase gene
849 cluster in *Drosophila*. Gene 2008, doi:10.1016/j.gene.2008.01.002.
850 50. Julien E, Coulon-Bublex M, Garel A, Royer C, Chavancy G, Prudhomme J-C, et al.
851 Silk gland development and regulation of silk protein genes. In: Gilbert LI, editor.
852 Comprehensive molecular insect science. Amsterdam: Elsevier; 2005;369-384.
853 51. Akai H. The silk gland. In: Akai H, editor. Ultrastructural morphology of insects.
854 Tokyo: University of Tokyo press; 1976;57-114.
855 52. Takasu Y, Hata T, Uchino K, Zhang Q. Identification of Ser2 proteins as major
856 sericin components in the non-cocoon silk of *Bombyx mori*. Insect Biochem Mol
857 Biol. 2010. doi:10.1016/j.ibmb.2010.02.010.
858 53. Bello B, Horard B, Couble P. The selective expression of silk-protein-encoding
859 genes in *Bombyx mori* silk gland. Bull Inst Pasteur. 1994;92;81-100.
860 54. Akai H. Porous cocoon filaments – Their characteristic and formation. Int J wild
861 silkmoth & silk. 2005;10:57-74.
862 55. Bolger AM, Lohse M, Usadel B. Trimmomatic: a flexible trimmer for Illumina
863 sequence data. Bioinformatics. 2014. doi:10.1093/bioinformatics/btu170.
864 56. Kim D, Paggi JM, Park C, Bennett C, Salzberg SL. Graph-based genome alignment
865 and genotyping with HISAT2 and HISAT-genotype. Nat Biotechnol. 2019.
866 doi:10.1038/s41587-019-0201-4.

867 57. Pertea M, Kim D, Pertea GM, Leek JT, Salzberg SL. Transcript-level expression
868 analysis of RNA-seq experiments with HISAT, StringTie and Ballgown. Nat Protoc.
869 2016. doi:10.1038/nprot.2016.095.
870 58. gffcompare [https://ccb.jhu.edu/software/stringtie/gffcompare.shtml].
871 59. Bray NL, Pimentel H, Melsted P, Pachter L. Near-optimal probabilistic RNA-seq
872 quantification. Nat Biotechnol. 2016. doi:10.1038/nbt.3519.
873 60. TIBCO Spotfire [http://spotfire.tibco.com/better-world-donation-program/].
874 61. Morpheus [https://software.broadinstitute.org/morpheus].
875 62. R Core Team (2019). R: A language and environment for statistical computing. R
876 Foundation for Statistical Computing, Vienna, Austria.
877 63. R Core Team (2020). R: A language and environment for statistical computing. R
878 Foundation for Statistical Computing, Vienna, Austria.
879 64. TransDecoder [https://transdecoder.github.io/].
880 65. Altschul SF, Madden TL, Schäffer AA, Zhang J, Zhang Z, Miller W, et al. Gapped
881 BLAST and PSI-BLAST: a new generation of protein database search programs.
882 Nucleic Acids Res. 1997. doi:10.1093/nar/25.17.3389.
883 66. Tabunoki H, Ono H, Ode H, Ishikawa K, Kawana N, Banno Y, et al. Identification of
884 key uric acid synthesis pathway in a unique mutant silkworm *Bombyx mori* model of
885 Parkinson's disease. 2013. doi:10.1371/journal.pone.0069130.
886 67. Kinsella RJ, Kähäri A, Haider S, Zamora J, Proctor G, Spudich G, et al. Ensembl
887 BioMarts: a hub for data retrieval across taxonomic space. Database (Oxford).
888 2011. doi:10.1093/database/bar030.
889 68. Zhou Y, Zhou B, Pache L, Chang M, Khodabakhshi AH, Tanaseichuk O, et al.
890 Metascape provides a biologist-oriented resource for the analysis of systems-level
891 datasets. Nat Commun. 2019. doi:10.1038/s41467-019-09234-6.
892 69. SilkBase [http://silkbase.ab.a.u-tokyo.ac.jp/cgi-bin/index.cgi].

70. KAIKObase [https://kaikobase.dna.affrc.go.jp/].

71. TogoTV [https://togotv.dbcls.jp/pics.html].

72. Creative Commons [http://creativecommons.org/licenses/by/4.0/deed.en].

897 # Tables

898 Table 1. Samples for RNA-seq and run accession IDs.

899

Sample	SRA Run ID	Strain	Sex	Reference
ASG-1,2,3	DRR186474,DRR186475,DRR186476	p50T	Male	This study
MSG_A-1,2,3	DRR186477,DRR186478,DRR186479	p50T	Male	This study
MSG_M-1,2,3	DRR186480,DRR186481,DRR186482	p50T	Male	This study
MSG_P-1,2,3	DRR186483,DRR186484,DRR186485	p50T	Male	This study
PSG-1,2,3	DRR186486,DRR186487,DRR186488	p50T	Male	This study
FB-1,2,3	DRR186489,DRR186490,DRR186491	p50T	Male	This study
MG-1,2,3	DRR186492,DRR186493,DRR186494	p50T	Male	This study
MT-1,2,3	DRR186495,DRR186496,DRR186497	p50T	Male	This study
TT-1,2,3	DRR186498,DRR186499,DRR186500	p50T	Male	This study
OV-1,2,3	DRR186501,DRR186502,DRR186503	p50T	Female	This study
BN_TT-1,2,3	DRR068893,DRR068894,DRR068895	o751	Male	[25]
BN_FB-1,2,3	DRR095105,DRR095106,DRR095107	o751	Male	[27]
BN_MG-1,2,3	DRR095108,DRR095109,DRR095110	o751	Male	[26]
BN_MT-1,2,3	DRR095111,DRR095112,DRR095113	o751	Male	[27]
BN_SG-1,2,3	DRR095114,DRR095115,DRR095116	o751	Male	[27]

900

Figures

Fig. 1

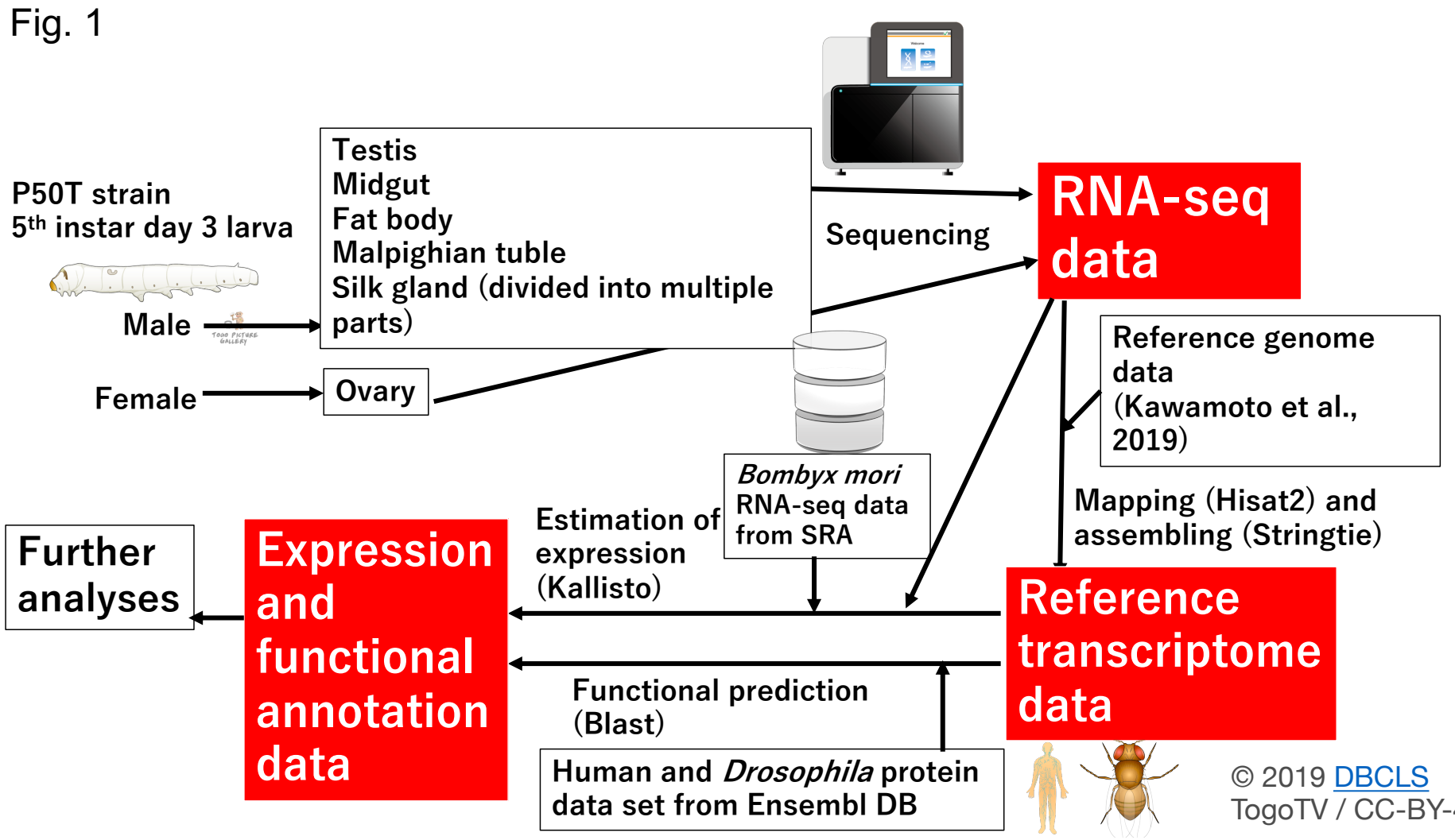

© 2019 DBCLS
TogoTV / CC-BY-4.0

Fig. 2

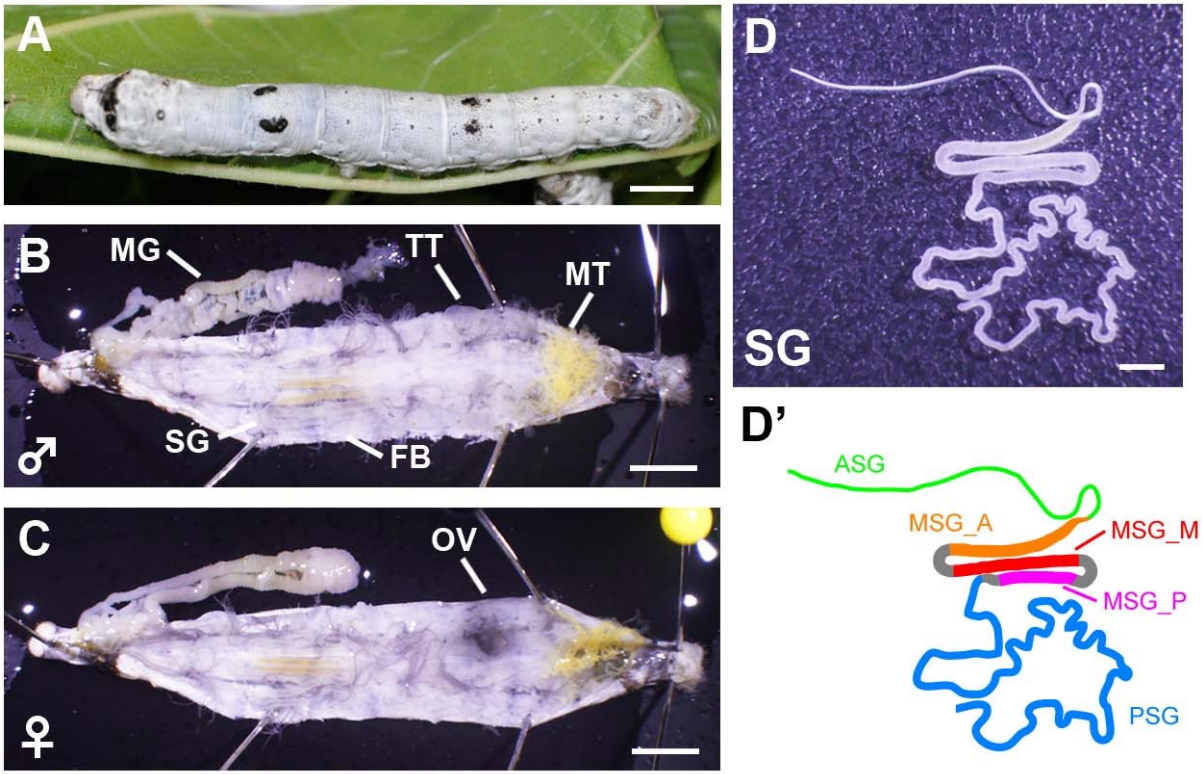

Fig. 3

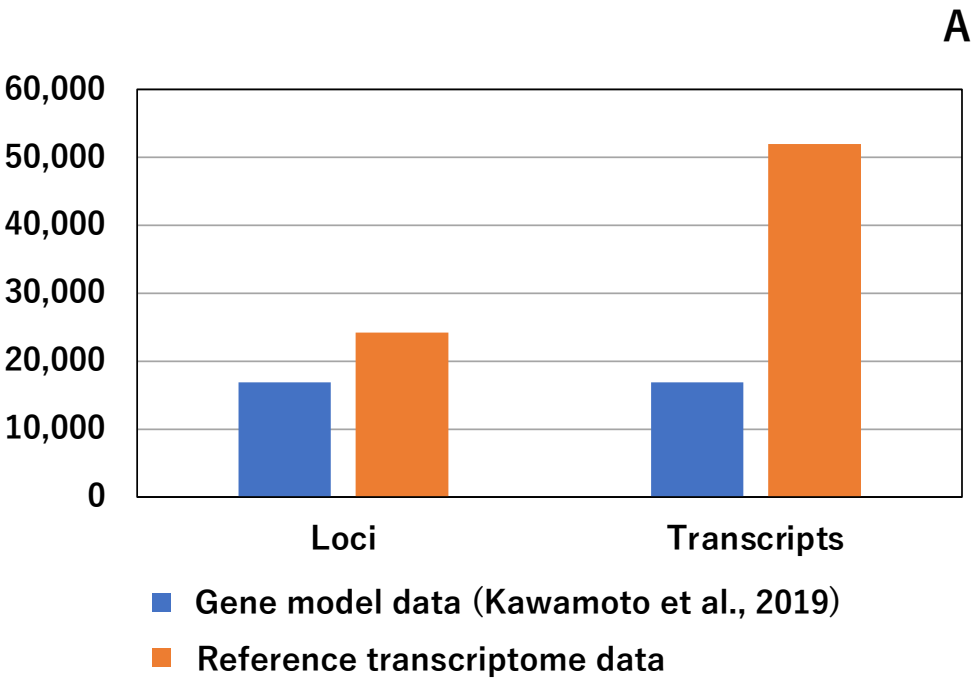
A
60,000
50,000
40,000
30,000
20,000
10,000
0
Loci
Transcripts
Gene model data (Kawamoto et al., 2019)
Reference transcriptome data

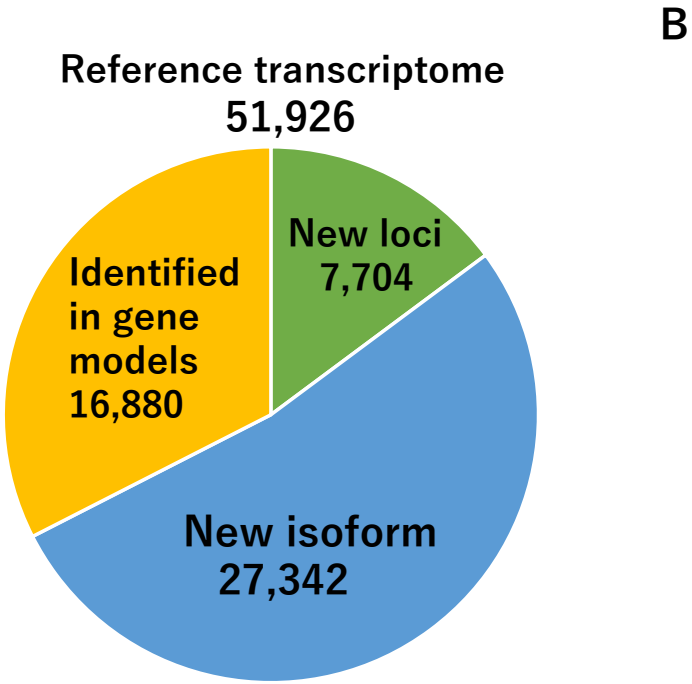
B
Reference transcriptome
51,926
New loci
7,704
Identified
in gene
models
16,880
New isoform
27,342

Fig. 4

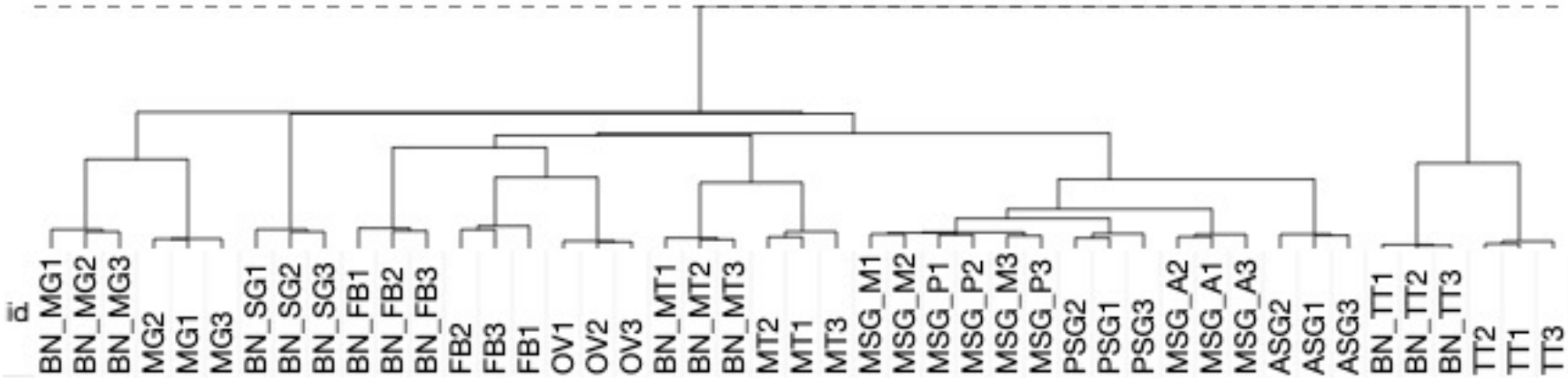
id
BN_MG1
BN_MG2
BN_MG3
MG2
MG1
MG3
BN_SG1
BN_SG2
BN_SG3
BN_FB1
BN_FB2
BN_FB3
FB2
FB3
FB1
OV1
OV2
OV3
BN_MT1
BN_MT2
BN_MT3
MT2
MT1
MT3
MSG_M1
MSG_M2
MSG_P1
MSG_P2
MSG_M3
MSG_P3
PSG2
PSG1
PSG3
MSG_A2
MSG_A1
MSG_A3
ASG2
ASG1
ASG3
BN_TT1
BN_TT2
BN_TT3
TT2
TT1
TT3

Fig. 5

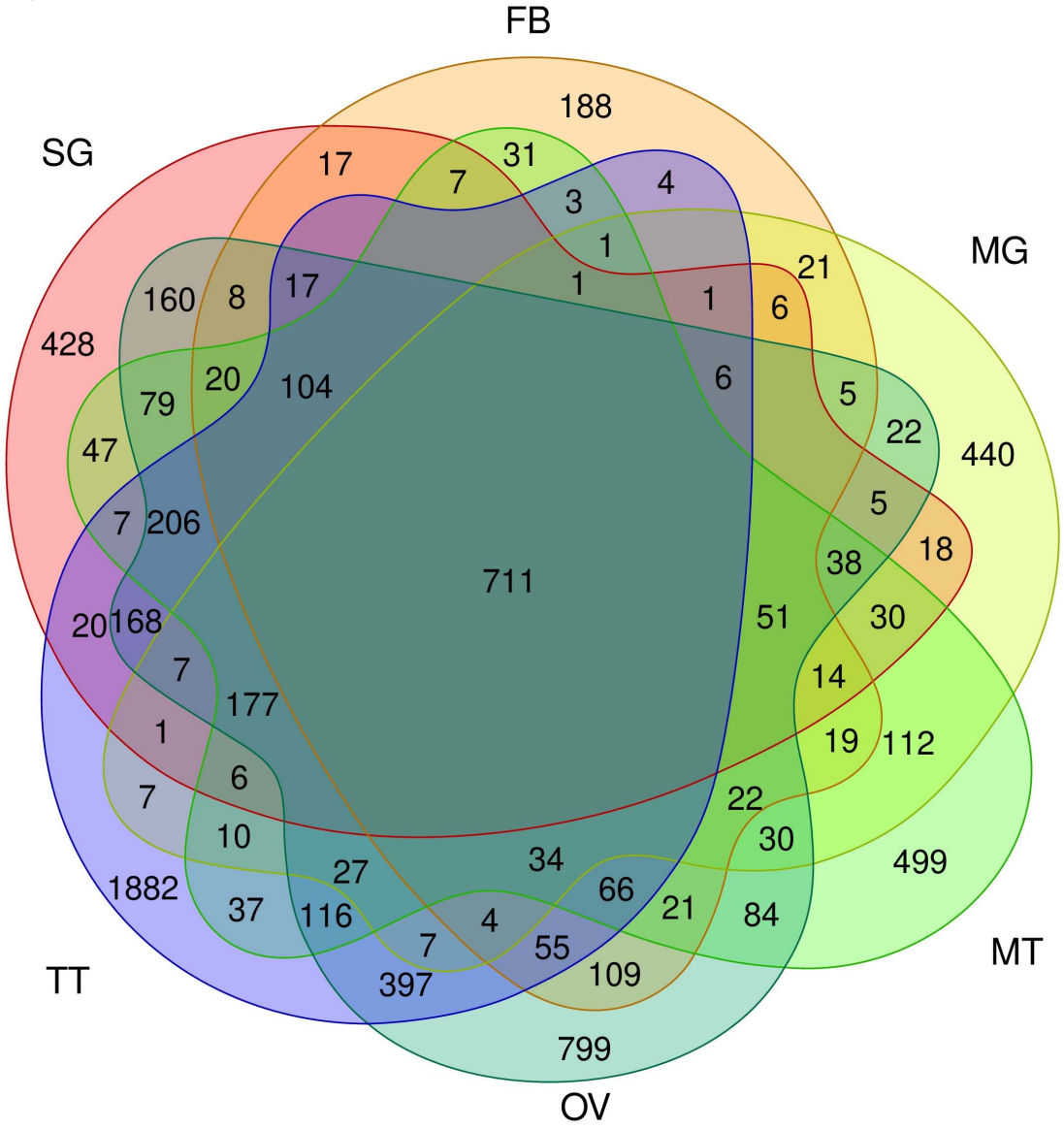
FB
SG
MG
TT
MT
OV
188
17
31
7
3
4
1
21
160
8
17
1
1
6
428
20
104
6
5
79
22
440
47
5
7
206
18
38
711
51
30
20
168
7
14
177
1
19
112
6
7
22
10
30
34
499
27
66
1882
37
116
21
84
4
7
55
109
397
799

Fig. 6

(A) TT

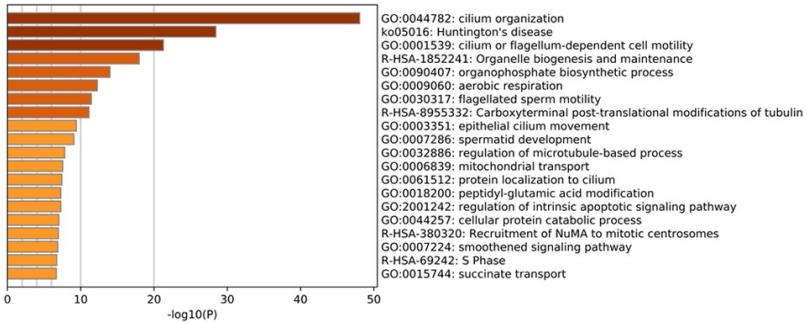
GO:0044782: cilium organization
ko05016: Huntington's disease
GO:0001539: cilium or flagellum-dependent cell motility
R-HSA-1852241: Organelle biogenesis and maintenance
GO:0090407: organophosphate biosynthetic process
GO:0009060: aerobic respiration
GO:0030317: flagellated sperm motility
R-HSA-8955332: Carboxyterminal post-translational modifications of tubulin
GO:0003351: epithelial cilium movement
GO:0007286: spermatid development
GO:0032886: regulation of microtubule-based process
GO:0006839: mitochondrial transport
GO:0061512: protein localization to cilium
GO:0018200: peptidyl-glutamic acid modification
GO:2001242: regulation of intrinsic apoptotic signaling pathway
GO:0044257: cellular protein catabolic process
R-HSA-380320: Recruitment of NuMA to mitotic centrosomes
GO:0007224: smoothened signaling pathway
R-HSA-69242: S Phase
GO:0015744: succinate transport
0
10
20
30
40
50
-log10(P)

(B) OV

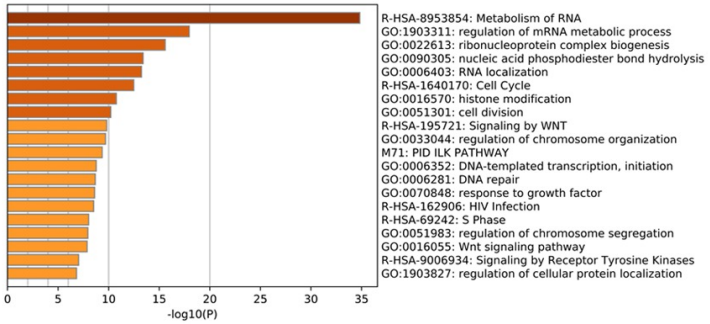
R-HSA-8953854: Metabolism of RNA
GO:1903311: regulation of mRNA metabolic process
GO:0022613: ribonucleoprotein complex biogenesis
GO:0090305: nucleic acid phosphodiester bond hydrolysis
GO:0006403: RNA localization
R-HSA-1640170: Cell Cycle
GO:0016570: histone modification
GO:0051301: cell division
R-HSA-195721: Signaling by WNT
GO:0033044: regulation of chromosome organization
M71: PID ILK PATHWAY
GO:0006352: DNA-templated transcription, initiation
GO:0006281: DNA repair
GO:0070848: response to growth factor
R-HSA-162906: HIV Infection
R-HSA-69242: S Phase
GO:0051983: regulation of chromosome segregation
GO:0016055: Wnt signaling pathway
R-HSA-9006934: Signaling by Receptor Tyrosine Kinases
GO:1903827: regulation of cellular protein localization
0
5
10
15
20
25
30
35
-log10(P)

Fig. 7

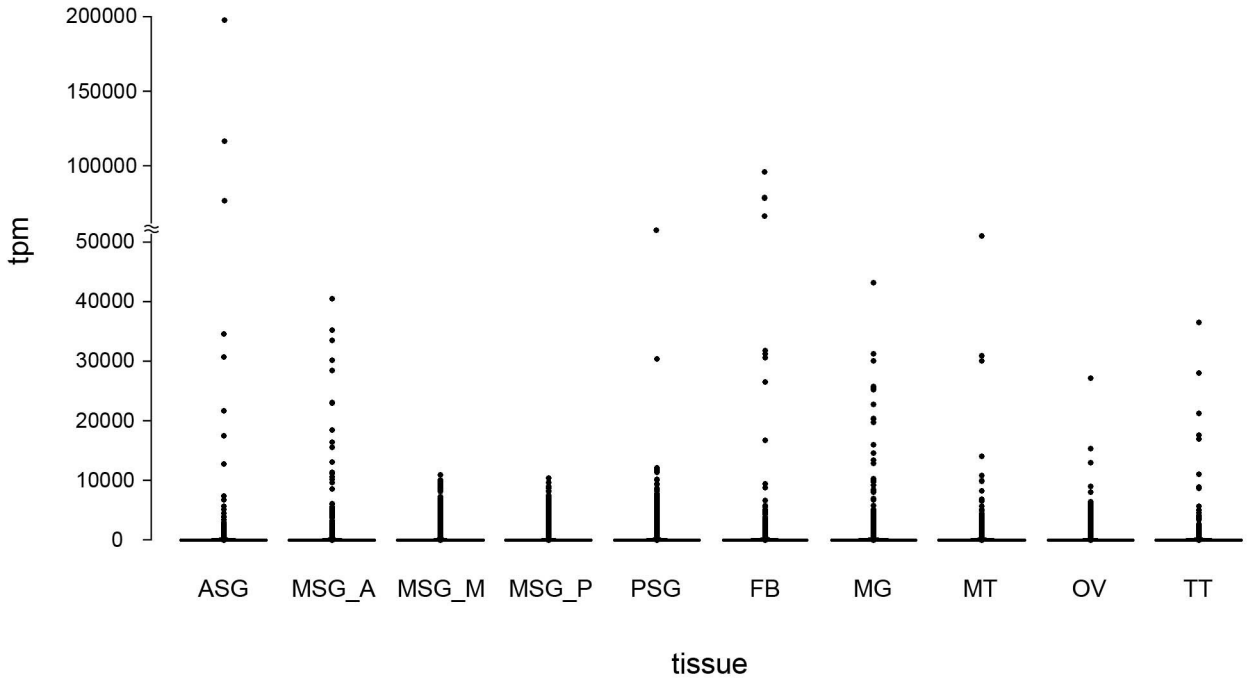
200000
150000
100000
50000
40000
30000
20000
10000
0
tpm
ASG
MSG_A
MSG_M
MSG_P
PSG
FB
MG
MT
OV
TT
tissue

Fig. 8

(A)

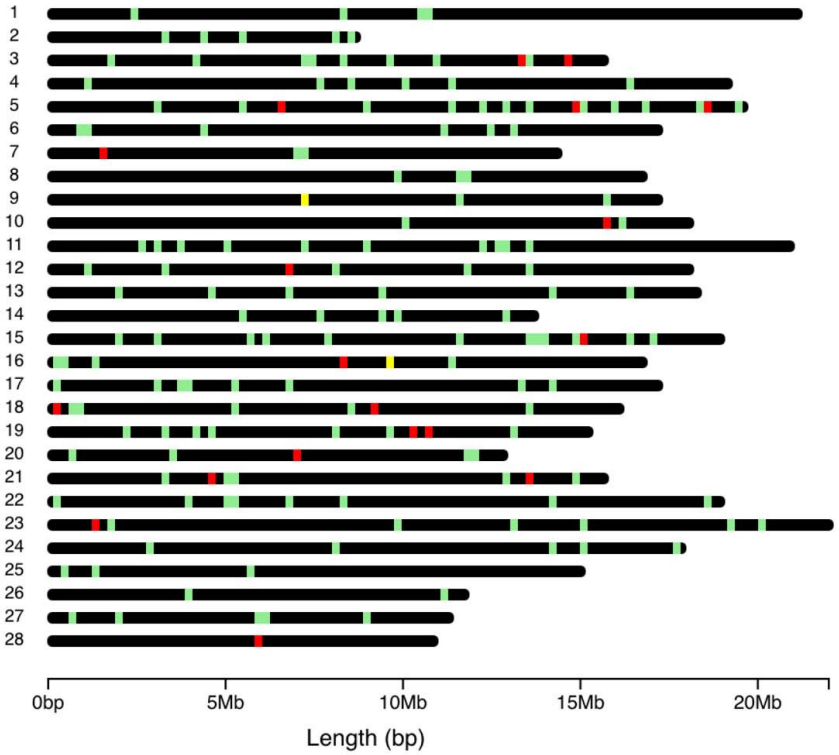
1
2
3
4
5
6
7
8
9
10
11
12
13
14
15
16
17
18
19
20
21
22
23
24
25
26
27
28
0bp
5Mb
10Mb
15Mb
20Mb
Length (bp)

(B)

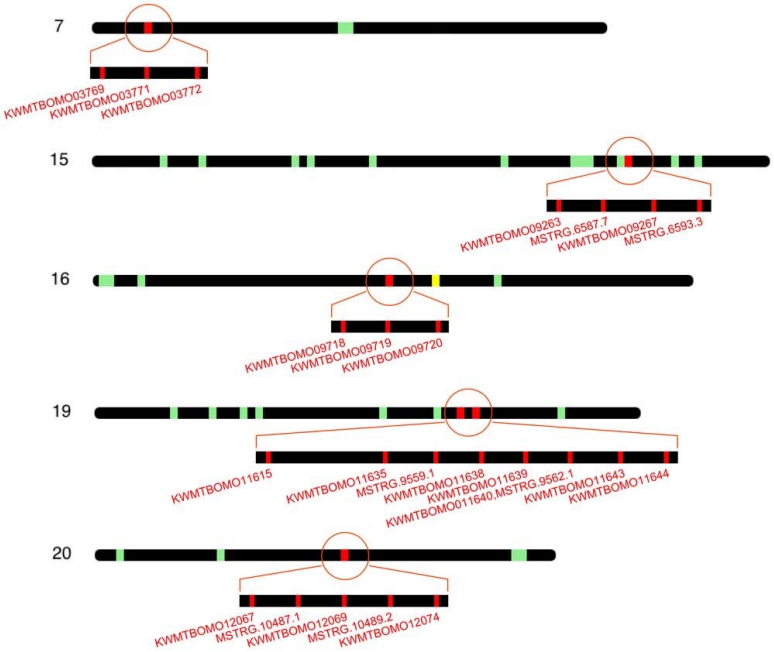
7
KWMTBOMO03769
KWMTBOMO03771
KWMTBOMO03772
15
KWMTBOMO09263
MSTRG.6587.7
KWMTBOMO09267
MSTRG.6593.3
16
KWMTBOMO09718
KWMTBOMO09719
KWMTBOMO09720
19
KWMTBOMO11615
KWMTBOMO11635
MSTRG.9559.1
KWMTBOMO11638
KWMTBOMO11639
KWMTBOMO011640,MSTRG.9562.1
KWMTBOMO11643
KWMTBOMO11644
20
KWMTBOMO12067
MSTRG.10487.1
KWMTBOMO12069
MSTRG.10489.2
KWMTBOMO12074

Fig. 9

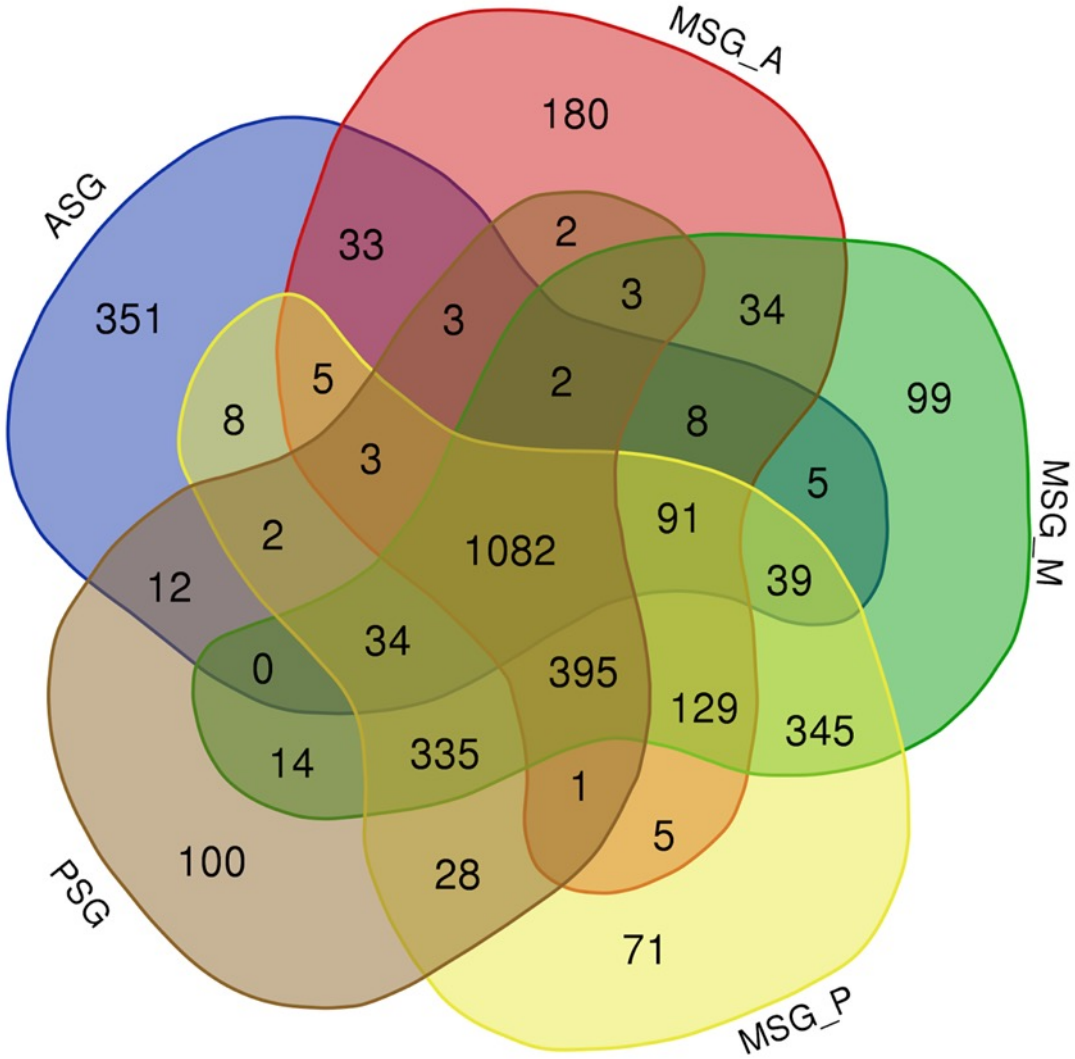
MSG_A
180
ASG
351
33
2
3
3
34
5
2
99
8
8
3
5
91
2
1082
MSG_M
12
39
34
0
395
129
345
14
335
1
5
100
28
PSG
71
MSG_P

Fig. 10

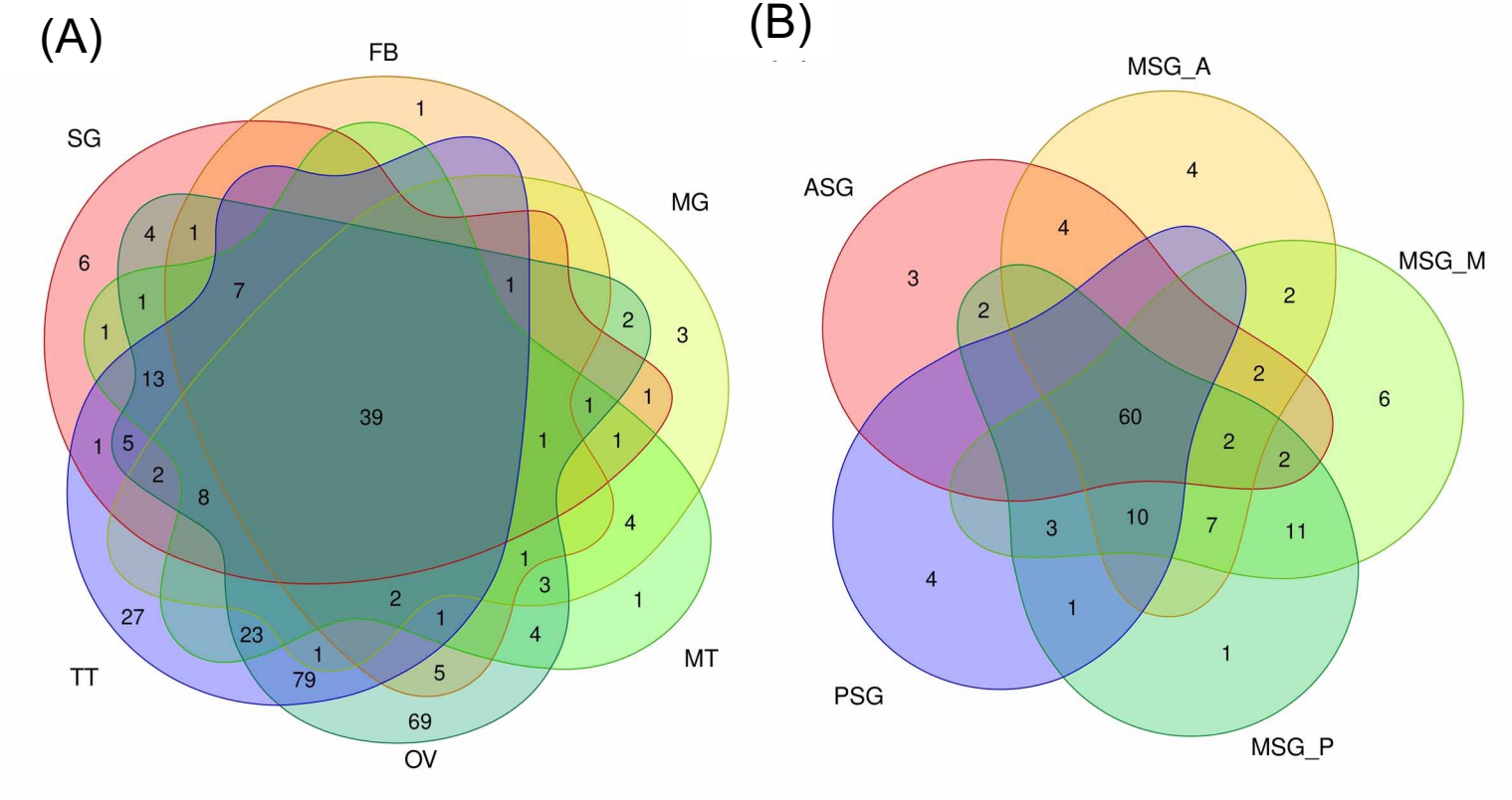
(A)
FB
SG
MG
TT
MT
OV
1
6
4
1
7
1
1
2
3
13
39
1
1
1
5
1
1
2
8
4
1
3
2
1
27
23
4
1
79
5
69
(B)
MSG_A
ASG
MSG_M
PSG
MSG_P
4
4
3
2
2
2
6
60
2
2
3
10
7
11
4
1
1